Conf-751116--6

MASTER

REJECTION OF RADIO-FREQUENCY NOISE WITH A WIDE-BAND DIFFERENTIAL PREAMPLIFIER AND SOLID-SHIELDED COAXIAL INPUT CABLES*

R. S. Burns J. T. De Lorenzo

Oak Ridge National Laboratory
Oak Ridge, Tennessee 37830

*Research sponsored by the Energy Research and Development Administration under contract with the Union Carbide Corporation.

REJECTION OF RADIO-FREQUENCY NOISE WITH A WIDE-BAND DIFFERENTIAL PREAMPLIFIER AND SOLID-SHIELDED COAXIAL INPUT CABLES*

R. S. Burns J. T. De Lorenzo

Oak Ridge National Laboratory
Oak Ridge, Tennessee 37830

Radio-frequency signals simulating electrical interference ranging from 50 kHz to 50 MHz were applied to the shields of the input cable system (two solid-shielded, mineral-insulated cables ∿6 m long) of a wide-band (∿60 MHz) differential preamplifier to determine the common-mode rejection. Results show that differences in electrical properties and shielding characteristics of the two input coaxial cables along with end effects produced by an unbalanced sensor severely degrade the rejection capability of the differential preamplifier. At 1 MHz, the common-mode rejection without input cables is ∿ -70 dB; this is reduced to ∿ -10 dB when measured with the rf signal applied to the surface of the input cable shields.

Measurements of the shielding characteristics of the input cables showed resonances at test frequencies >2 MHz. A ferrite core was installed in the input assembly to increase the impedance of the shields and to permit termination of the coaxial line consisting of the input cable shields and the protective metal conduit for the input cables. This assembly eliminated all resonances below 20 MHz. The increased impedance also reduced the amplitude of the shield currents, resulting in an increase in the shielding effectiveness of the input cables without affecting the signal transmission of the cables.

Introduction

Differential current-pulse preamplifiers have been developed for use with fission counters as input devices as part of in-vessel, low-level flux monitors in future liquid-metal fast breeder reactors (LMFBRs).[1] Their balanced input, coupled with balanced input cables, should reduce false counts from electrical interference--a common problem for low-level flux monitors. The problem is particularly acute for a current-pulse system because of the extremely small signals (∿50 μV) and large bandwidth requirements (∿15 MHz).

The effectiveness of these preamplifiers to reject electrical pickup was measured previously.[1,2] The results were informative, showing that a differential preamplifier is superior to a preamplifier with a single-ended input. The rf generator used in these earlier measurements (a vacuum-tester coil) produced an rf spectrum, however, which was not suited to a characterization of rejection as a function of frequency. Also, the measurements were not completely relevant because they did not include an input cable assembly which is intended for the LMFBR application.

This work uses sinusoidal rf signals to reveal how the differences in the electrical properties and shielding characteristics of the two coaxial input cables and the end effects produced by an unbalanced sensor influence the common-mode rejection (CMR) of the differential preamplifier and input cable system. The common-mode signal is an rf current applied to the outer surface of the shields of two solid-shielded, mineral-insulated (MI) input cables, 6 m in length. CMR measurements were made with a balanced resistor sensor to isolate the influence of shielding characteristics from those caused by an unbalanced sensor.

The shielding characteristic of each shield was measured to determine if the differences could explain the CMR performance with the balanced sensor. Finally, CMR measurements were made with an unbalanced sensor to determine if there was any further degradation of the CMR.

The measurements of shielding characteristics which required rf signal currents of known amplitude in the shields of the input cables showed resonances at test frequencies >2 MHz. These resonances develop because the shields of the two input cables and the protective metal conduit which encloses the input cables form a coaxial line that is shorted at the preamplifier end. A ferrite core was used to raise the impedance of the shields of the input cables and to permit a termination of this line and eliminate all resonances below 20 MHz. Additionally, this increased impedance will reduce the amplitude of rf shield currents and improve the shielding effectiveness of the input cables without affecting their signal transmission properties.

Test Apparatus

All tests were made with the apparatus shown in Fig. 1 or with slight modifications to the apparatus. Plastic spacers kept the two input cables evenly spaced within a flexible stainless steel conduit. This arrangement closely resembles the normal application of the differential preamplifier with a fission counter in a nuclear reactor. The stainless steel conduit substituted for the containment which normally is used to protect the fission counter and cables from the reactor environment.

A three-element capacitor network mounted in a small steel box simulated a fission detector with asymmetrical floating electrodes driving differential outputs. This capacitor network was replaced by the balanced resistor network for portions of the work.

A common-mode rf current was produced in the shields of the input cables by applying an rf voltage to the cable system comprising the input cable shields and stainless steel conduit. A resistor network was inserted to obtain an impedance match between this cable and the impedance of the rf generator. The stainless steel conduit was connected at each end to galvanized steel boxes which enclosed both the simulated counter and the differential preamplifier to complete the shielding for the counter-input cable-preamplifier system.

A final shield consisting of additional galvanized steel boxes and a galvanized steel flexible conduit enclosed the entire test setup to prevent rf radiation throughout the test area, which would have contaminated the test data.

*Research sponsored by the Energy Research and Development Administration under contract with the Union Carbide Corporation.

An rms voltmeter was used to monitor the output of the rf generator and the rf voltage applied to the input cable shields and stainless steel conduit cable system. A spectrum analyzer was used as a sensitive, selective rf voltmeter.

Effects of the Electrical Properties of the Input Cables on CMR

To establish a reference for the CMR of the differential preamplifier and the two 6-m lengths of input cables, the CMR of the preamplifier alone was determined by applying an rf voltage directly to the positive and negative inputs. The conventional expression for CMR is given as

$$CMR(dB) = -20 \log_{10}(V_{CMR} A_{vd}/V_{od}) ,$$

where V_{CMR} is the common-mode rf voltage, V_{od} is the differential preamplifier output voltage, and A_{vd} is the preamplifier differential voltage gain. A_{vd} can be measured by applying V_{CMR} separately to the positive and negative inputs and measuring the corresponding output voltages, $V_{o(+)}$ and $V_{o(-)}$. This permits A_{vd} to be expressed as $A_{vd} = [V_{o(+)} + V_{o(-)}]/V_{CMR}$. With this expression substituted in the above CMR equation, a new expression is obtained which is used to calculate the CMR here and throughout this paper:

$$CMR(dB) = -20 \log_{10} \frac{V_{o(+)} + V_{o(-)}}{V_{od}} .$$

It is important to recognize that the amplitude of the common-mode signal does not appear in this expression.

The CMR of the preamplifier alone is given in Fig. 2, curve A. With V_{CMR} applied through two 6-m lengths of MI cables, the CMR performance is as shown in Fig. 2, curve B. As a comparison, the CMR measurement was repeated with the two MI cables replaced with two 6-m lengths of RG-58/U (50-Ω coaxial cable); the data are shown in Fig. 2, curve C.

At 1 MHz, the data in Fig. 2 show that the CMR for the MI cables is ∿20 dB less than for the RG-58/U cables and ∿26 dB less than for the preamplifier alone. Most of this CMR loss for the MI cables is due to *differences* in the resistance of the center conductor (∿10 Ω for a 6-m length). The MI cables were manufactured by SODERN in France, and consist of a stainless steel cladded, copper center conductor (∿0.25 mm diam) and a cladded outer conductor (∿4 mm diam). The outer copper conductor is cladded with stainless steel on both the inner and outer surfaces. Measurements of its characteristic impedance with a time-domain reflectometer indicated a value of 52 Ω.

Shielding Characteristics

Transfer Impedance as a Measure of Shielding Characteristics

The shielding characteristic of a coaxial cable can be expressed by the magnitude of its transfer impedance per unit length.[3] Figure 3 shows a basic scheme for measuring the transfer impedance. A shield current, I_s, of known magnitude and frequency applied to the outer surface of the shield of the coaxial cable is related to a voltage, V_c, developed across the inner surface by the transfer impedance of the shield as follows:

$$Z_T = V_c/I_s \ell ,$$

where ℓ is the length of the cable. In measurements of Z_T, length ℓ is kept short (∿1 m) to avoid resonances over the range of test frequencies.

Measurements of this type were made earlier[4] of a 1-m-long sample of the 4-mm MI cable used in these tests; the results are plotted in Fig. 4. Also plotted in Fig. 4 are calculations for an all-stainless-steel version of this cable and calculated transfer impedances of the cladded type. The magnitude of the transfer impedance approaches the dc resistance per unit length of the shield as the test frequency approaches dc. This can be seen in the differences in the Z_T of the two cables shown in Fig. 4. The cladded cable with a lower dc resistance exhibits smaller values of Z_T. As the test frequency is increased, the skin effect phenomenon reduces the voltage developed across the inner surface, giving lower values of transfer impedance. This is also seen in Fig. 4 by the lower values of Z_T as the frequency of measurement is increased.

Measurement of Transfer Impedance of the Input Cable Shields

The transfer impedance of each MI cable of the input cable system was measured with a test setup that can be described from Fig. 1. For this test, the capacitor network was removed, and the balanced resistor network was substituted.* To measure the transfer impedance of one cable shield, the preamplifier section associated with the opposite cable was deactivated without affecting the input impedance of the preamplifier. As shown, the test current was applied to the shields of the input cable and was returned to the rf generator through the stainless steel flexible conduit.

To calculate the Z_T of the cable, one must know both the magnitude of this shield current and the voltage, V_c, which it generates. To calculate the shield current, the cable system comprising the input cable shields and stainless steel conduit which encloses the input cables must be considered. This cable is ∿6 m long, with one end shorted. The resistor network shown between the generator and this cable is used to create a termination of this cable# at the rf generator end.

The method of calculating I_s and V_c (and, hence, Z_T) can be seen from Fig. 5a. The current from the rf generator is $2I_s$, which supplies a value of I_s for each cable shield. The return path of the shield current is through the ground path of the circuit as shown. The current $2I_s$ can be calculated from the rf voltages, V_I and V_S, existing at the terminal ends of the resistor network and the value of the three resistors R_1, R_2, and R_3. The resistors R_D were 50 Ω ± 0.1% and were selected to provide a termination of the input cable at the sensor end. With R_A also equal to the characteristic impedance of the input cable, reflections were minimized during the measurement.

The value of the voltage V_c can be derived from the voltage across the input to the preamplifier, V_a. If the input impedance of this preamplifier is R_a (which matches the characteristic impedances of the input cable), then $V_c = (V_a/R_a)(R_a + R_D)$. For the work here, R_a was 50.0 Ω.

---

*The balanced nature of this network is not needed here, but will be used in later tests. These resistors were selected to be within ±0.1%.

#The characteristic impedance of this cable was measured to be ∿66 Ω .

The values of Z_T for the two input cable shields are shown in Fig. 6, along with the Z_T measurement from a 1-m-long sample of the input cable (from Fig. 4). The occurrence of resonances in the measurement with the 6-m lengths is apparent above 2 MHz. These resonances develop from the shorted coaxial line properties of the cable system comprising the input cable shields and stainless steel conduit. Data to be shown later demonstrate how these resonances can be partially suppressed by the termination of this cable with the use of a ferrite core.

The differences in the transfer impedance of the two input cable shields at 1 MHz (1.12×10^{-3} and 1.04×10^{-3}) would account for a CMR of $\sim$ -22 dB.* Measured CMR data to be described in the next section show a CMR of $\sim$ -17 dB at 1 MHz for this case.

Effects of Shield Characteristics of the Input Cables on CMR

For these measurements, the resistor termination was substituted for the capacitor network, as shown in Fig. 1. These resistors essentially eliminated any effects of an unbalanced sensor on the CMR measurements.

The rf generator output voltage was adjusted to give an amplitude of shield current I_S which would produce a differential output above the noise level of the preamplifier. Attention was given to the amplitude of the common-mode signals (particularly at resonances of I_S) developed at the input of the preamplifier to avoid any possible overloading of the input stages. At each frequency, three output signals were obtained with the spectrum analyzer. One output, $V_{O(+)}$, was measured with the negative half of the preamplifier deactivated, while still maintaining the input impedance, R_a. Another output, $V_{O(-)}$, was measured with the positive half similarly deactivated. The third output, V_{Od}, was measured with both inputs active. The CMR was then calculated, using the expression described previously.

The results of this CMR test is given in the column headed "Resistor Termination" in Table 1. At 1 MHz the CMR is indicated as $\sim$ -17 dB. This represents a degradation of $\sim$30 dB from a CMR determined purely from electrical properties of the two input cables. Most of the degradation can be explained on the basis of differences in the shielding characteristic (transfer impedance) of the shields of the two input cables. Measurements on transfer impedance from the preceding section indicate that at 1 MHz the CMR, based on differences in transfer impedance alone, gives a CMR value of $\sim$ -22 dB.

An examination of the CMR data also reveals that by nature of the CMR process, the resonances of the shield current (which clearly exist above 2 MHz, as evidenced by the Z_T measurements) do not appear in the data of Table 1.

Effects of Sensor Impedance on CMR

Two-electrode fission counters of cylindrical geometry will have different values of capacitances from each electrode to the outer shell (C_2 and C_3 of Fig. 1). (For a developmental, high temperature fission counter, the interelectrode capacitances were C_2 = 120 pF, C_1 = 330 pF, and C_3 = 10 pF.) These differences in the values of C_2 and C_3 will create an imbalance and further degrade the CMR of the differential input system.

The CMR was measured for this capacitor network, using the same procedure applied previously. The results obtained are given in the last column of Table 1. For frequencies ranging from 0.5 to 20 MHz, the values of the CMR were lower than those obtained for the balanced resistive network. As an example, at 1 MHz the CMR was measured as $\sim$ -11 dB, which is 6 dB lower than that obtained with the balanced resistor network.

The effect of the unbalanced capacitor network on the CMR can be partially explained by the consideration of Fig. 5b and the expression for the preamplifier input voltage, V_A, as

$$V_A = V_c[R_A/(R_A + Z_D)] .$$

This expression is obtained from an earlier relationship for V_c in the description of transfer impedance, with Z_D substituted for R_D. Here, Z_D is the impedance developed by the capacitor network across one end of the input cable. For the input cable connected to the positive input of the preamplifier, Z_D is C_3 in shunt with the series combination of C_1 and R_A.* For the input cable connected to the negative input of the preamplifier, Z_D is C_2 in shunt with the series combination of C_1 and R_A.#

The application of the above equation to calculate V_A for each cable [$V_{A(+)}$ and $V_{A(-)}$] at 1 MHz yields a CMR of -11 dB. Previously described CMR measurements with the balanced resistor network showed a value of -17 dB at this test frequency. If an additional 12 dB of degradation (as calculated) is produced by the capacitor network, the total CMR should be -5 dB, whereas measurements with the capacitor network (Table 1) indicate a value of -11 dB. An explanation for this and results of other measured data is given below.

The measured values of the CMR from 25 to 50 MHz show an unexpected superior performance to that obtained with the balanced resistor network. An explanation can be made by the influence of C_1 in the development of the two voltages $V_{A(+)}$ and $V_{A(-)}$. This capacitor will couple signals from $V_{c(+)}$ and $V_{c(-)}$ into the opposite input cable. At the higher test frequencies, its reactance is sufficiently small such that both V_c generators are nearly equally coupled to both input cables, yielding an improvement of CMR performance.

At the lowest test frequency of 50 kHz, the CMR performance with the capacitor network appears to be better than that of the balanced resistor network, and also superior to the CMR measurement obtained for the electrical property study. This apparent improvement can be explained by experimental error. At this low value of the test frequency, the reactance of the capacitors is high, yielding extremely small values for both $V_{A(+)}$ and $V_{A(-)}$. False values due to preamplifier noise could easily distort the data.

Exact Expression for V_A with Z_D as a Capacitor

The simple expression for V_A in the preceding section is only valid for a coaxial cable length such that $\beta\ell$ is << 1, where β is the phase constant of the

*CMR = -20 $\log_{10}$ {[(1.12 + 1.04)/2]/[1.12 - 1.04]}.

*This neglects the shunting effect of C_2 across R_A and is valid for frequencies below $\sim$26 MHz.

#This neglects the shunting effect of C_3 across R_A and is valid for frequencies below $\sim$300 MHz.

test frequency. With a method used by Harrison,[5] an exact expression can be obtained for Z_D, which is a capacitor, with the aid of Fig. 7.

The induced current, I_c, is expressed as

$$I_c = \int_0^{\ell} [I_s Z_T/(Z + R_A)]\, dx ,$$

where Z is the impedance at the elemental length dx seen looking toward the impedance Z_D. The voltage V_A is then taken as $I_c R_A$.

If we assume that the input cable is a lossless transmission line, Z can be expressed as[6]

$$Z(\ell - x) = R_A \{[Z_D \cos \beta(\ell - x) + jR_A \sin \beta(\ell - x)] / [R_A \cos \beta(\ell - x) + jZ_D \sin \beta(\ell - x)]\} ,$$

where x is the distance from the preamplifer terminated end. With substitution for Z, $Z_D = -j/\omega C_D$, and integrating, we obtain

$$I_c = \frac{I_s Z_T}{\beta R_A [(R_A \omega C_D)^2 + 1]} \left\{ \frac{\beta\ell}{2} [(R_A \omega C_D)^2 + 1] + \frac{\sin(2\beta\ell)}{4} [(R_A \omega C_D)^2 - 1] - \frac{\cos(2\beta\ell)}{2} R_A \omega C_D + \frac{R_A \omega C_D}{2} - j \left[- \frac{\sin(2\beta\ell)}{2} R_A \omega C_D - \frac{\cos(2\beta\ell)}{4} \times [(R_A \omega C_D)^2 - 1] + \frac{1}{4} [(R_A \omega C_D)^2 - 1] \right] \right\} ,$$

where ω is the angular velocity. Assuming $2\beta\ell << 1$ and taking only the first term of the series expansion of sin $(2\beta\ell)$ and cos $(2\beta\ell)$, we obtain

$$I_c = I_s Z_T/(Z_D + R_A) .$$

This expression assumes a constant value of I_s over the entire length of the cable, ℓ. When resonances occur, the CMR values will not be affected since the CMR is a ratio that is independent of I_s, but the shielding effectiveness of the input cables will be reduced.

Resonances of RF Currents on the Input Cable Shields

Input Cable Shield Resonances

Measurements to determine the transfer impedance of the shields of the input cables showed resonances at test frequencies above 2 MHz. These resonances can be explained by considering the shields of the input cables and the protective stainless steel flexible conduit as a shorted transmission line. If this line is assumed lossless, the impedance, Z_s, seen by the matching resistor network at the rf generator can be expressed[6] as

$$Z_s = | j Z_c \tan(2\pi f\ell/v_p) | ,$$

where Z_c is the characteristic impedance of the cable system comprising the input cable shields and stainless steel conduit, and v_p the cable propagation velocity. Resonant peaks ($Z_s \to \infty$) occur at $f = (2n + 1) \times v_p/4\ell$ (n = 0, 1, 2, ...), and nulls ($Z_s = 0$) occur at $f = nv_p/2\ell$ (n = 0, 1, 2, ...). If the propagation velocity of the cable is assumed 0.75c, where c is the speed of light, the first resonant peak for a 6-m cable is 9.2 MHz. Calculated and measured values for this impedance are given in Fig. 8. The effect of these resonances on the transfer impedance measurements (Fig. 6) shows peaks at ~9 and 27 MHZ and a null at ~18 MHz, and it is consistent with the resonances of Z_s as shown in Fig. 8.

Suppression of Resonances

Two inductors wound on a U-shaped ferrite core (Fig. 9) were used to raise the impedance of the shields of the two input cables at the preamplifier end. Two short lengths of RG-223/U coaxial cable, each ~0.5 m long, were used as the conductors for these inductors.* The rigidity of the solid-shielded input cables prevented their use to form the inductors. These inductors did not disturb the signal transmission properties of the input cables.

With the increased shield impedance, resistors R_{T1} and R_{T2} could be used to terminate the cable system comprising the input cable shields and stainless steel conduit. The value of the terminating resistance is the parallel combination of R_{T1} and R_{T2}, and it is equal to the characteristic impedance of the coaxial line.

The results with these inductors can be seen in Fig. 6, which shows the transfer impedance measurements on the input cable shields, and in Fig. 8, which shows the measurement of the input impedance of the input cable shields and conduit cable system.

In Fig. 6, the measurement of the transfer impedance of the shield of the input cable connected to the positive input of the preamplifier does not show the resonances previously seen. The eventual upturn of its transfer impedance is caused by the loss of permeability of the ferrite core at these higher frequencies and the possible influence of the loss of shielding caused by the braid of the short section of the RG-223/U cable.

In Fig. 8, the resonances of the input impedance of the input cable shields and conduit cable system are eliminated. The reduction of the impedance at the higher frequencies results from the loss of permeability of the ferrite core.

Conclusions

The common-mode rejection of the differential preamplifier is reduced by the imbalance of the electrical properties of the two, solid-shielded, mineral-insulated coaxial input cables. At 1 MHz the CMR is reduced ~26 dB. It is reduced further by differences in the shielding characteristics (transfer impedance) of the shields of the input cables, resulting in another ~30 dB loss at 1 MHz. CMR losses are also produced by effects of an unbalanced sensor, such as a two-electrode fission counter. At 1 MHz, differences in sensor impedance seen by the two input cables can cause ~6 dB additional loss. Greater losses by the imbalanced sensor are prevented by a compensating

*The inductance created by the shield of the coaxial cable was measured to be ~0.5 mH at 1 kHz.

effect caused by interaction between the two input cables through the capacitance existing between the electrodes.

The shields of the input cables and the metal conduit which enclose them form a coaxial line which is shorted at the preamplifier end. For a 6-m length of cable, resonances of shield currents are produced, with the first resonance occurring near 10 MHz. These resonances, if within the bandpass of the signal processing electronics, will reduce the shielding effectiveness of the cable.

Resonances can be eliminated below 20 MHz by the termination of this coaxial line with the use of a ferrite core. An additional benefit is derived by the reduction of shield current from the increased shield impedance so obtained.

References

1. "Current-Pulse Preamplifier for Fission Counters," *IEEE Trans. Nucl. Sci.* 21(1), 757 (1974).

2. J. T. De Lorenzo, W. T. Clay, and G. C. Guerrant, *Common-Mode and Integral Bias Tests with a Differential Current-Pulse Preamplifier*, ORNL-TM-4316 (1973).

3. J. T. De Lorenzo, "Measurements of Shielding Effectiveness of Coaxial and Two-Conductor Cables," *Rev. Sci. Instrum.* 43(1), 161 (1972).

4. D. P. Roux et al., *Neutron Sensor Development for Extreme Environments, Progress Report for Period Jan. 1, 1970 to June 30, 1972*, ORNL-TM-3959 (1972).

5. D. Harrison, "The Mechanism of Interference Pick-up in Cables and Electronic Equipment with Special Reference to Nuclear Power Stations," *Radio Electronic Engr.* 29(3), 149 (1965).

6. J. J. Karakash, *Transmission Lines and Filter Networks*, The Macmillian Co., New York, 1950.

Table 1. CMR(dB) of preamplifier

Frequency (MHz)	Preamplifier (Fig. 2)	MI Cable (Fig. 2)	MI Cable with Resistor Termination	MI Cable with Capacitor Termination
0.05	-35.1	-37.3	-26.4	-43.3
0.50	-70.6	-45.9	-17.6	-12.5
1.0	-72.0	-46.9	-16.9	-11.1
2.0	-70.8	-46.0	-19.3	-17.6
5.0	-62.3	-45.9	-17.8	-13.3
10.0	-58.0	-45.2	-6.1	-3.1
20.0	-50.8	-37.7	-15.1	-1.6
25.0	-46.0	-37.5	-16.5	-18.4
30.0	-45.2	-37.2	-14.3	-18.8
40.0	-40.4	-34.4	-8.9	-13.0
50.0	-32.0	-30.0	-20.0	-26.0

Figure Captions

Fig. 1. Test apparatus.

Fig. 2. CMR for preamplifier and input cables.

Fig. 3. Basic scheme for measurement of transfer impedance.

Fig. 4. Transfer impedance performance of solid-shielded MI cables.

Fig. 5. Equivalent circuit for the input cable system.

a. With resistor termination

b. With capacitor termination

Fig. 6. Values of Z_T for input cables with resistor terminations.

Fig. 7. Equivalent circuit for the input cable terminated with a capacitor.

Fig. 8. Resonances on the input cable system.

Fig. 9. Ferrite core installed between the preamplifier and input cables.

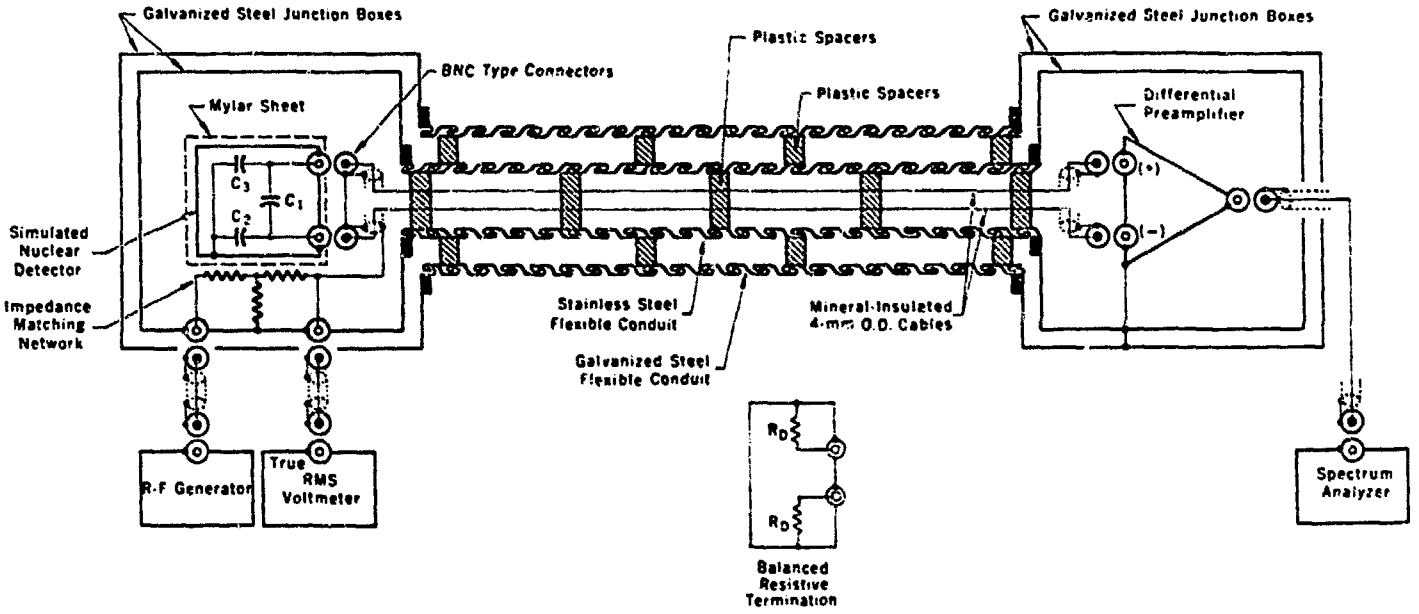
Galvanized Steel Junction Boxes
BNC Type Connectors
Mylar Sheet
Plastic Spacers
Plastic Spacers
Galvanized Steel Junction Boxes
Differential Preamplifier
C3
C1
C2
(+)
(-)
Simulated Nuclear Detector
Impedance Matching Network
Stainless Steel Flexible Conduit
Mineral-Insulated 4-mm O.D. Cables
Galvanized Steel Flexible Conduit
R-F Generator
True RMS Voltmeter
RD
RD
Balanced Resistive Termination
Spectrum Analyzer

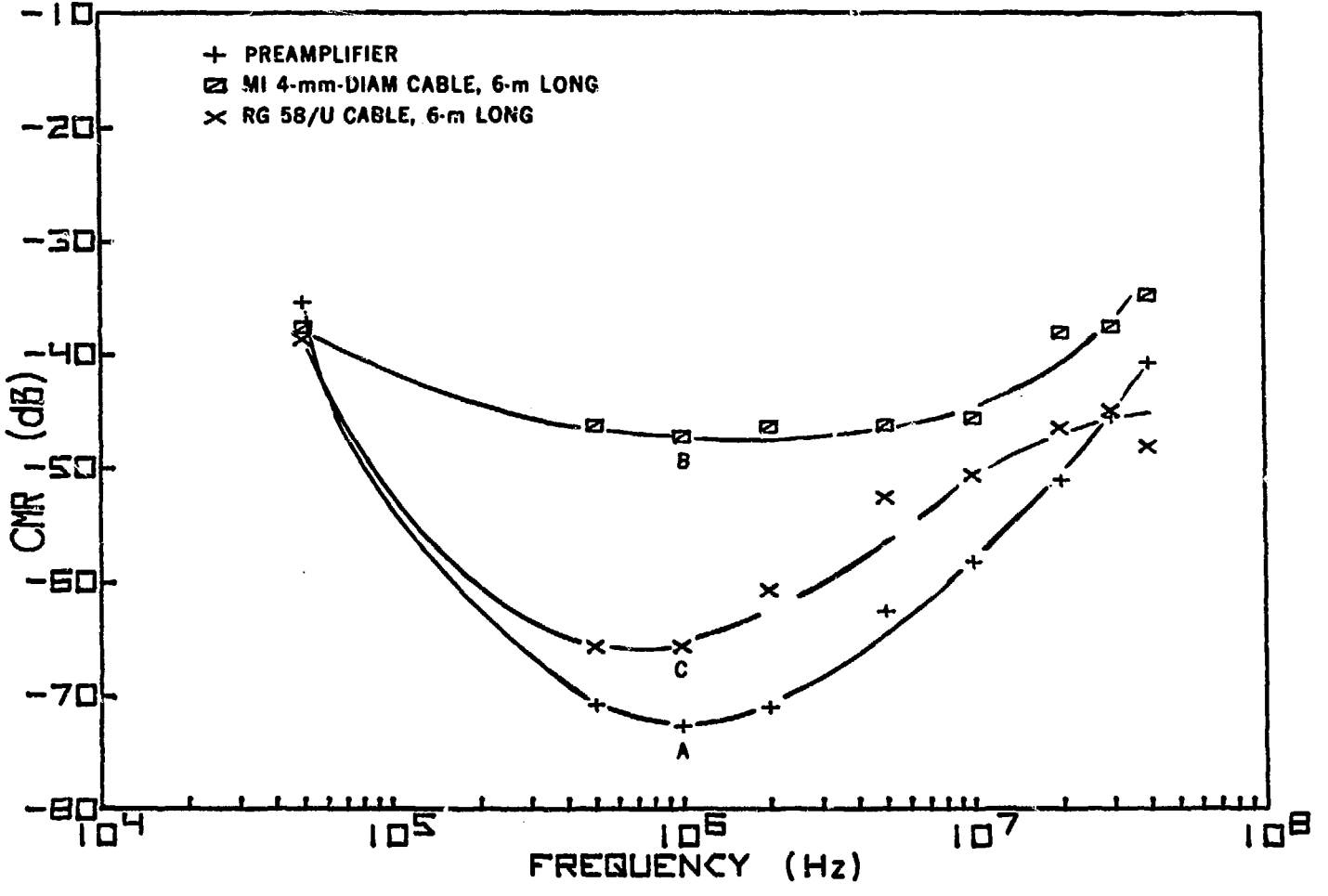
+ PREAMPLIFIER
⊠ MI 4-mm-DIAM CABLE, 6-m LONG
× RG 58/U CABLE, 6-m LONG
-10
-20
-30
-40
-50
-60
-70
-80
CMR (dB)
10⁴
10⁵
10⁶
10⁷
10⁸
FREQUENCY (Hz)
A
B
C

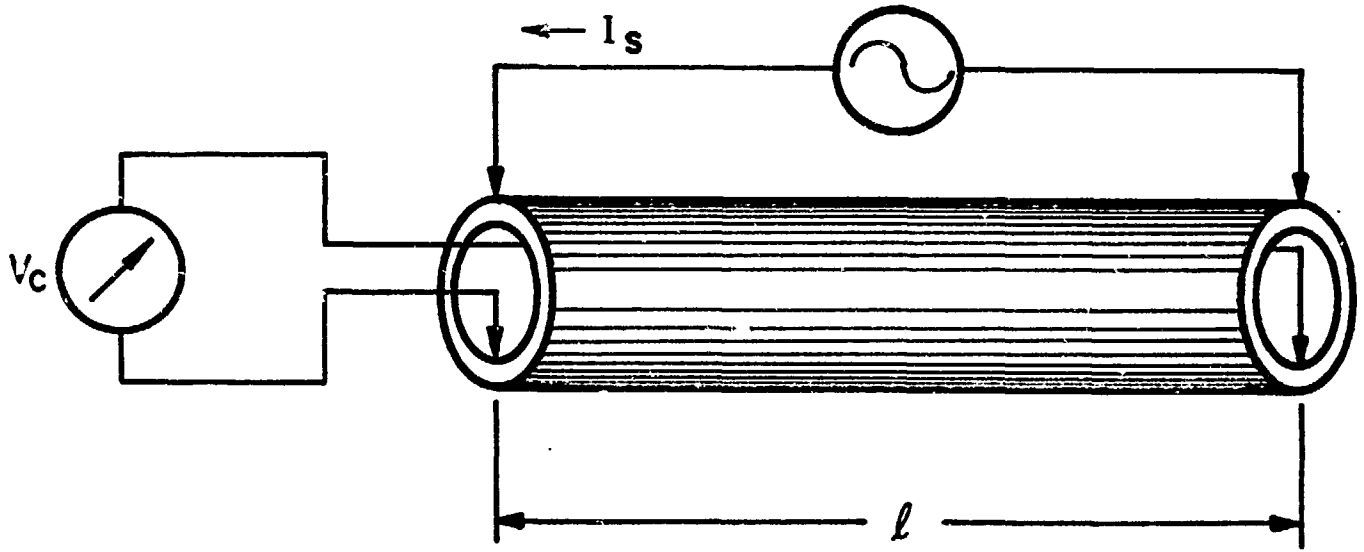

$$Z_T = \frac{V_c}{I_s \ell}$$

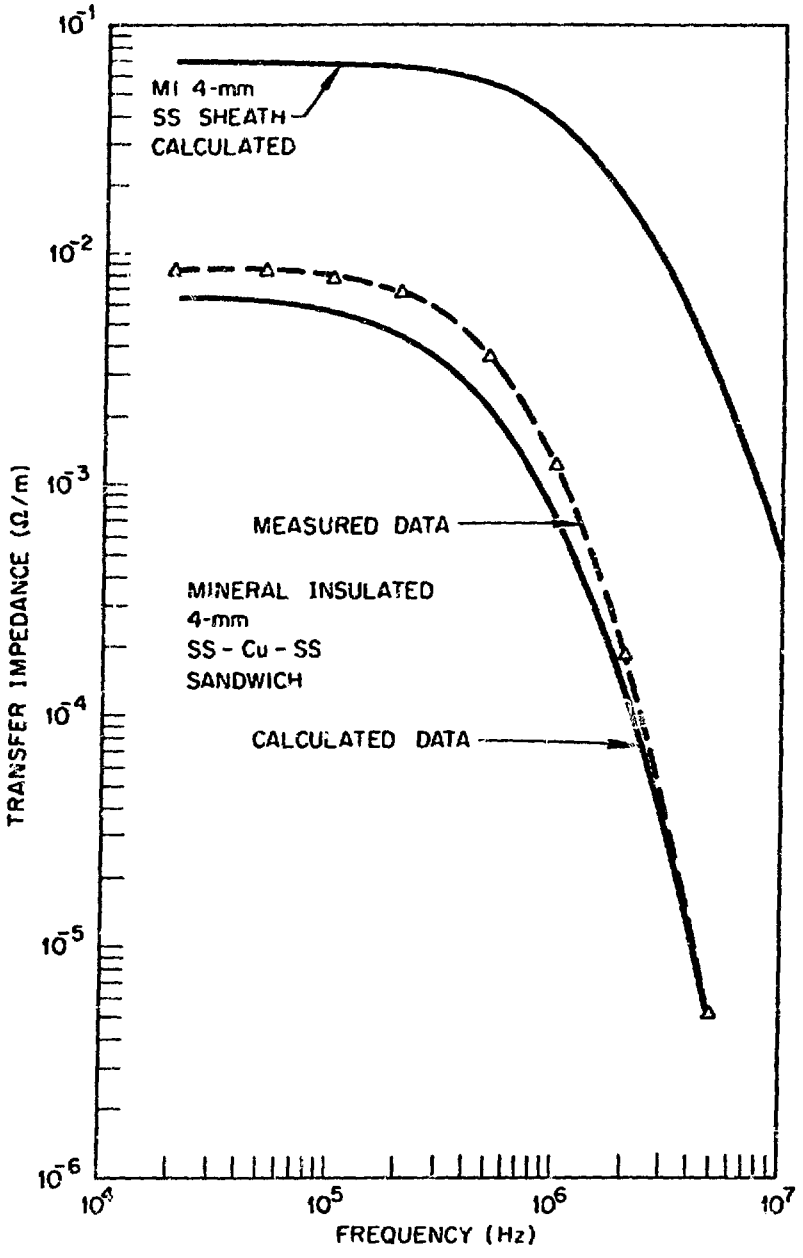
10^{-1}
10^{-2}
10^{-3}
10^{-4}
10^{-5}
10^{-6}
TRANSFER IMPEDANCE (Ω/m)
MI 4-mm
SS SHEATH
CALCULATED
MEASURED DATA
MINERAL INSULATED
4-mm
SS - Cu - SS
SANDWICH
CALCULATED DATA
10^{4}
10^{5}
10^{6}
10^{7}
FREQUENCY (Hz)

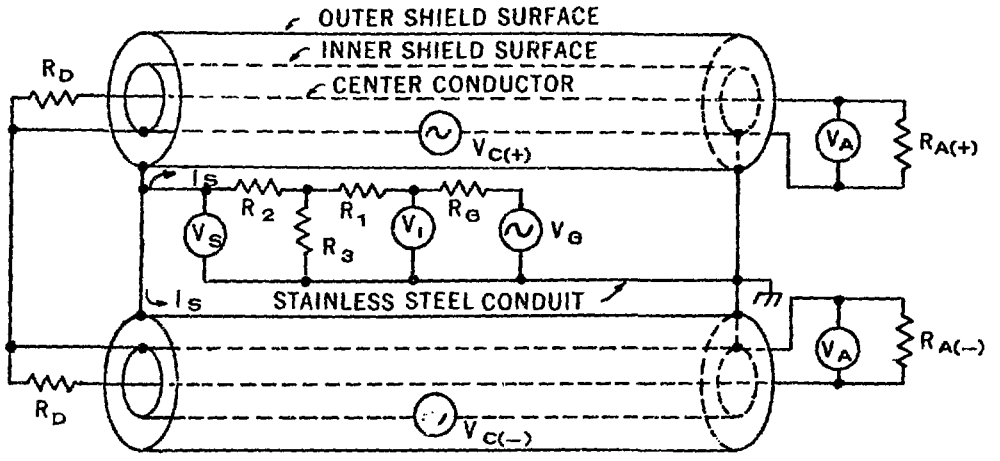
OUTER SHIELD SURFACE
INNER SHIELD SURFACE
CENTER CONDUCTOR
R_D
$V_{C(+)}$
I_S
R_2
R_1
R_G
V_S
R_3
V_I
V_G
V_A
$R_{A(+)}$
I_S
STAINLESS STEEL CONDUIT
V_A
$R_{A(-)}$
R_D
$V_{C(-)}$

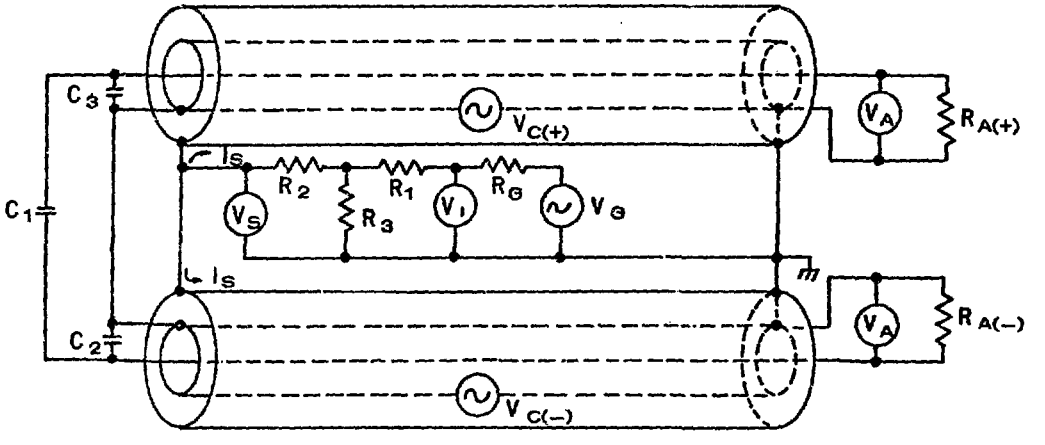
C_3
$V_{C(+)}$
V_A
$R_{A(+)}$
I_S
R_2
R_1
R_G
C_1
V_S
R_3
V_I
V_G
I_S
C_2
V_A
$R_{A(-)}$
$V_{C(-)}$

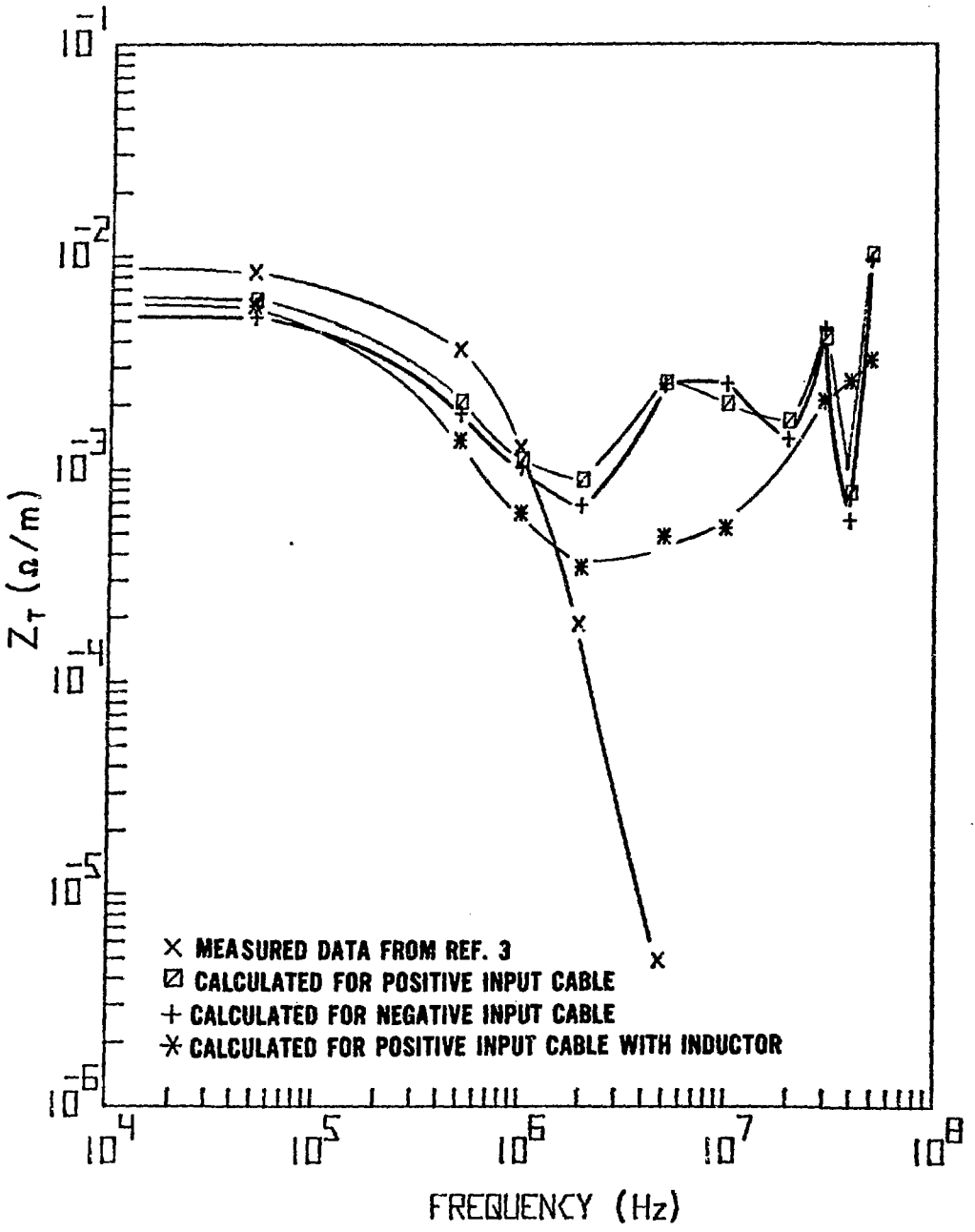
10^{-1}
10^{-2}
10^{-3}
10^{-4}
10^{-5}
10^{-6}
Z_T (Ω/m)
10^4
10^5
10^6
10^7
10^8
FREQUENCY (Hz)
× MEASURED DATA FROM REF. 3
⊠ CALCULATED FOR POSITIVE INPUT CABLE
+ CALCULATED FOR NEGATIVE INPUT CABLE
✳ CALCULATED FOR POSITIVE INPUT CABLE WITH INDUCTOR

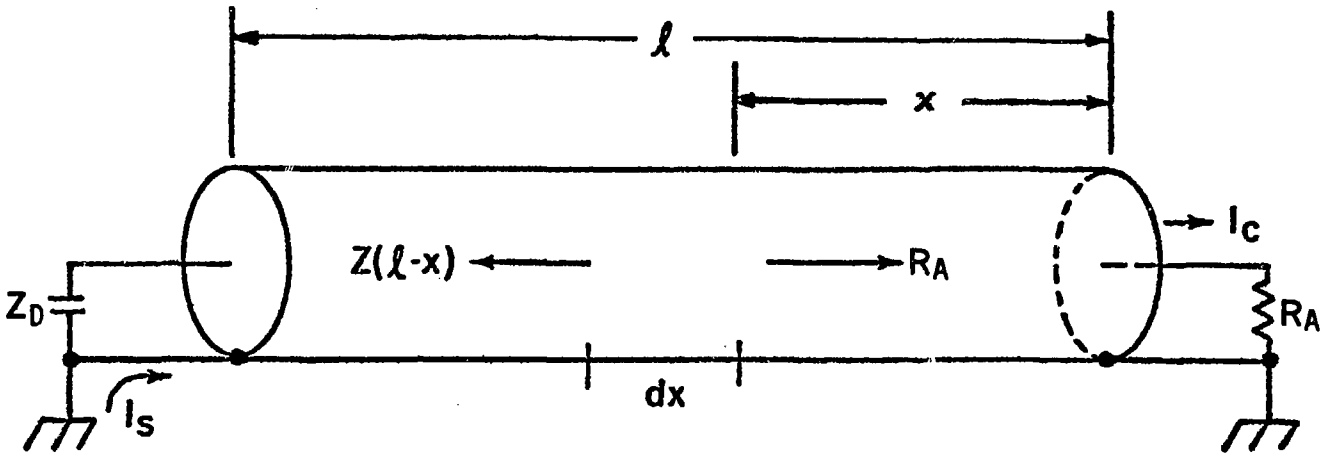
ℓ
x
Z(ℓ-x)
RA
Ic
ZD
RA
dx
Is

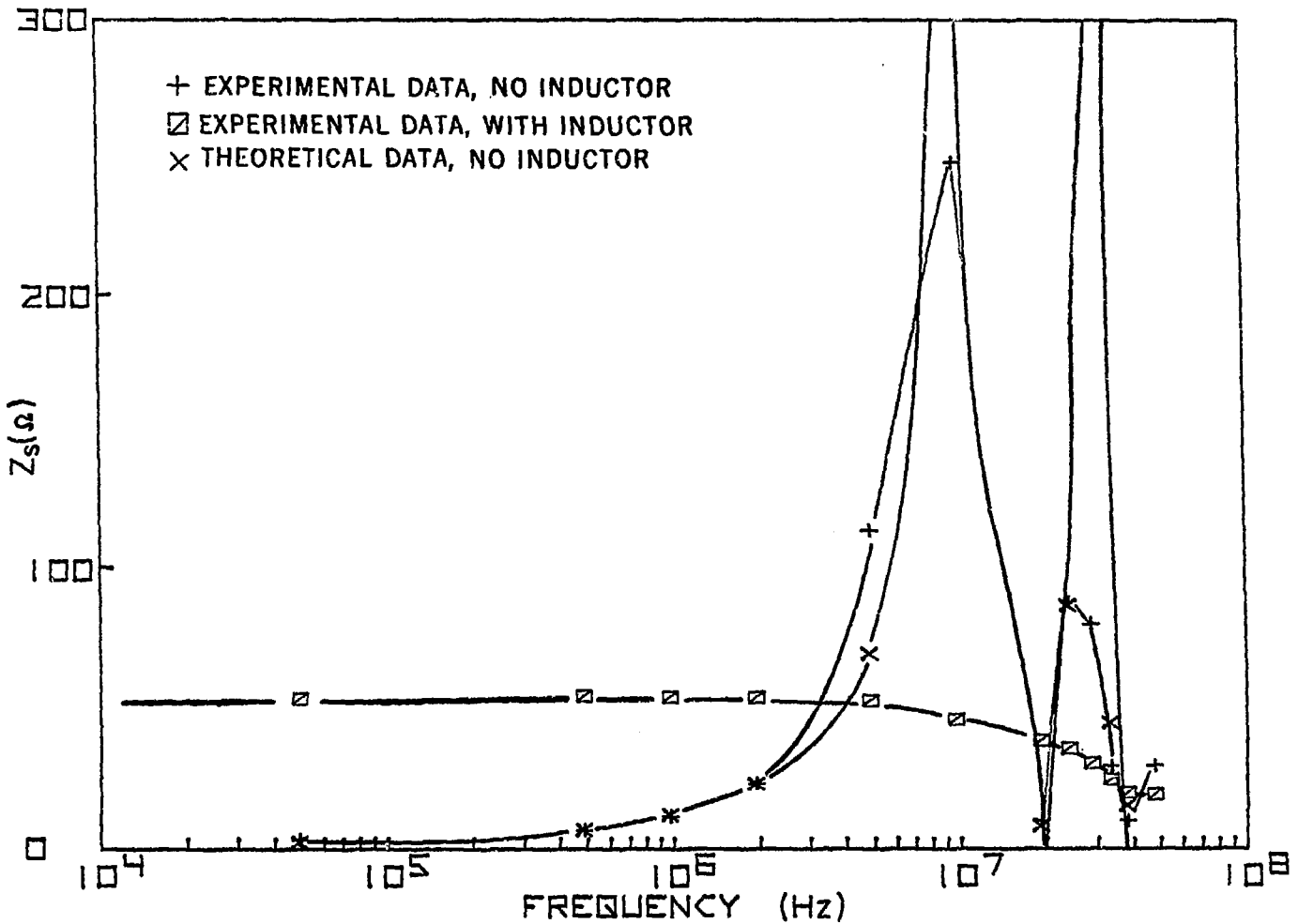
+ EXPERIMENTAL DATA, NO INDUCTOR
EXPERIMENTAL DATA, WITH INDUCTOR
× THEORETICAL DATA, NO INDUCTOR
300
200
100
0
$Z_s(\Omega)$
10^4
10^5
10^6
10^7
10^8
FREQUENCY (Hz)

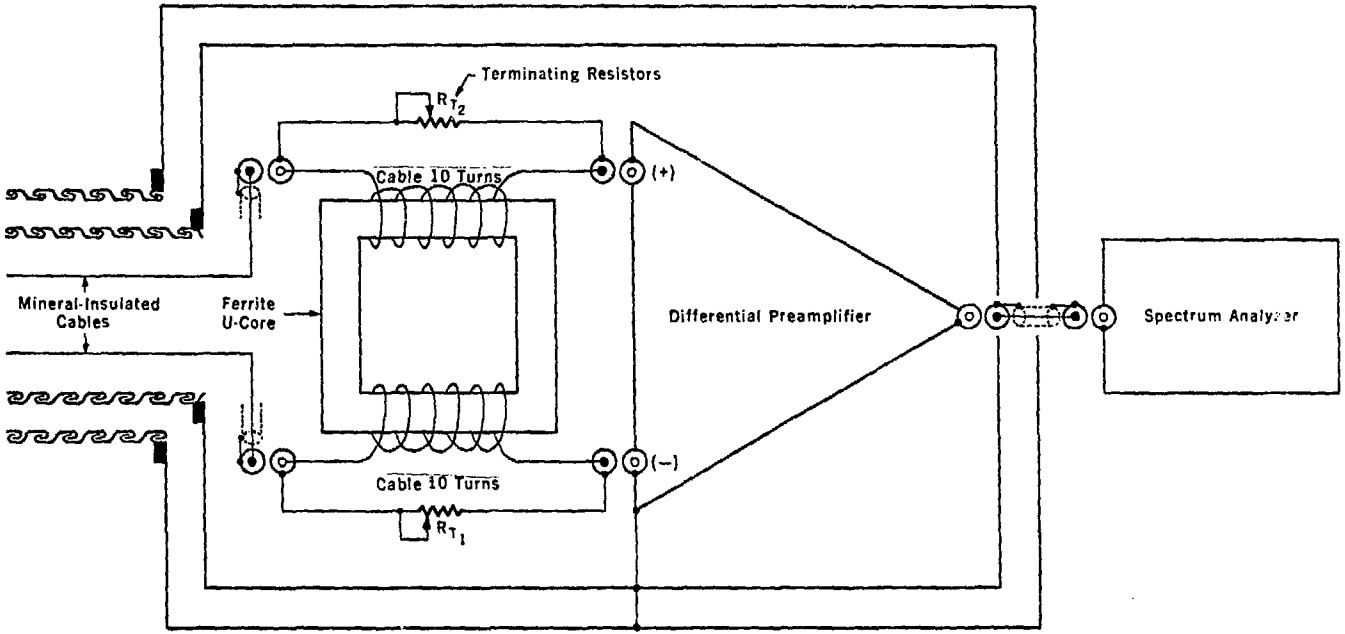
Terminating Resistors
R_{T_2}
Cable 10 Turns
(+)
Mineral-Insulated Cables
Ferrite U-Core
Differential Preamplifier
Spectrum Analyzer
Cable 10 Turns
(−)
R_{T_1}